Inventory of Supplemental Materials:

Figure S1

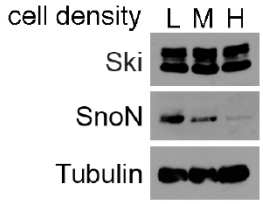

Figure S1, related to Figure 1. Ski abundance is not affected by cell density. The levels of SnoN and Ski in MCF10A cells cultured at low (L), medium (M) and high (H) cell density were measured by Western blotting. Tubulin was used as a loading control.

Figure. S2

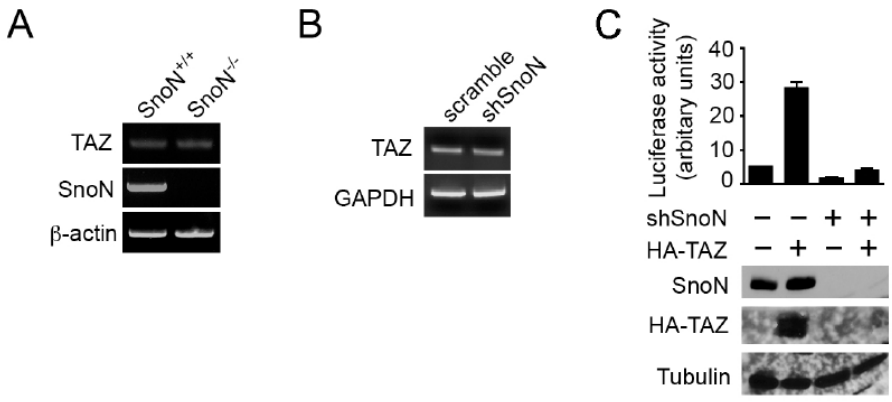

Figure S2, related to Figure 3&4. SnoN does not alter the mRNA levels of TAZ.
(**A**) SnoN does not alter the mRNA levels of TAZ. Total mRNA was extracted from pregnancy day 18.5 mammary glands of $SnoN^{+/+}$ and $SnoN^{-/-}$ mice and subjected to semi-qRT-PCR analyses. β-actin was used as a loading control in semi-qRT-PCR. (**B**) Reducing SnoN expression by shRNA did not affect the mRNA level of TAZ in MCF10A cells as analyzed by semi-qRT-PCR. GAPDH was used as a loading control. (**C**) Knocking down SnoN decreases TAZ-dependent transcription. The TAZ-dependent luciferase activity was measured in MEF cells expressing HA-TAZ in the presence or absence of shSnoN. Each data point represents mean ±SEM from two independent wells.

Figure S3:

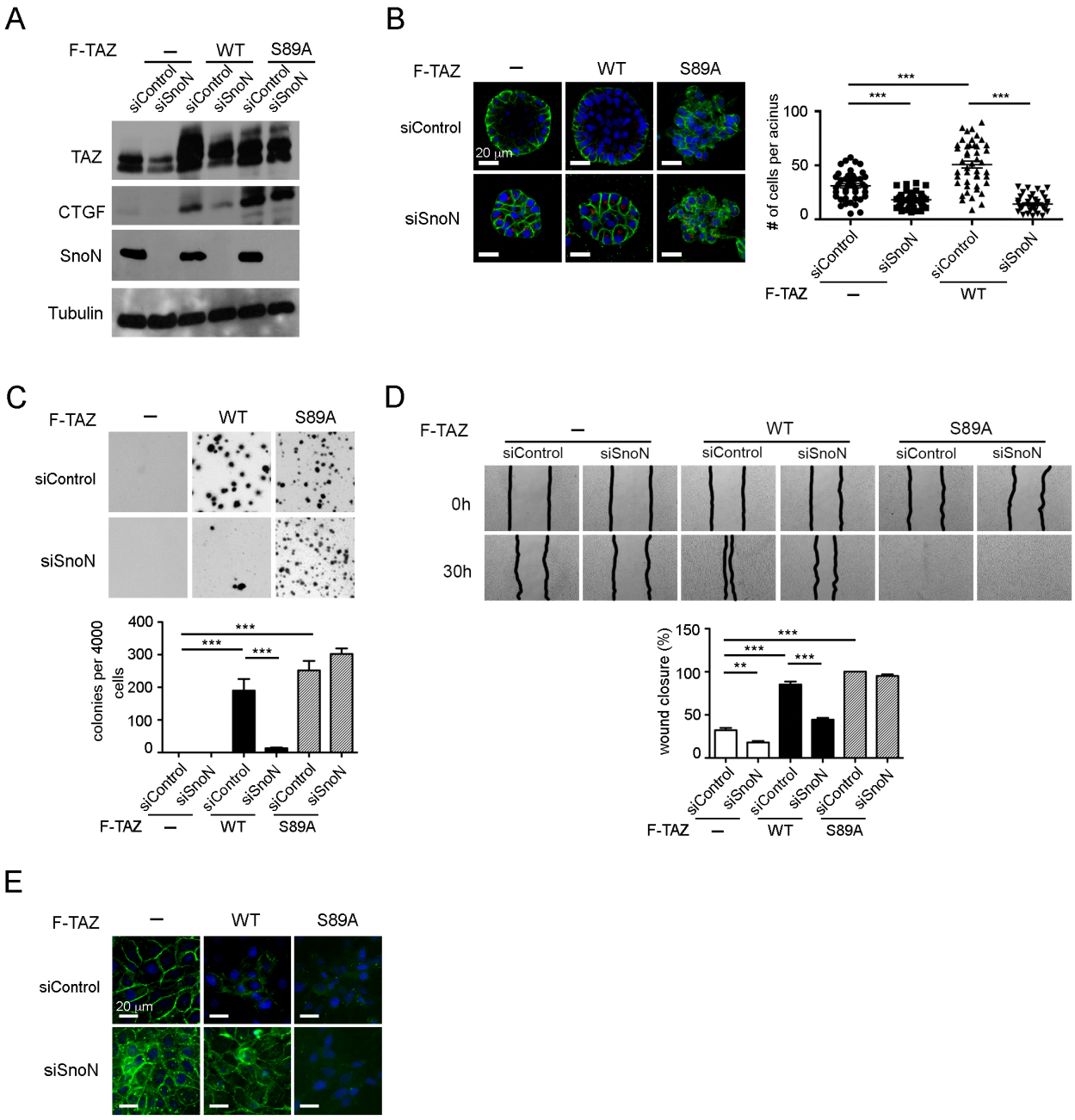

Figure S3, related to Figure 4. Reducing SnoN expression by siRNA impairs the transforming activities of TAZ.

(**A**) Western blotting analysis of TAZ and CTGF abundance in MCF10A cells expressing WT or S89A TAZ together with or without siSnoN. Tubulin was used as a loading control. (**B**) MCF10A cells stably expressing WT TAZ or TAZS89A together with or without siSnoN as indicated were cultured in 3D IrECM for six days before staining for α-integrin (green) and GM130 (red). Nuclei are stained with DAPI (blue). Left: Confocal images of a representative acinus. Scale bar, 20 μm. Right: The average size of acini was determined by the number of nuclei in each acinus and quantified in the graph. (**C-E**). Reducing SnoN

expression reversed transformation and EMT induced by WT TAZ, but not TAZ S89A. MCF10A cells stably expressing WT TAZ or TAZS89A together with or without siSnoN were subjected to Soft agar assay (**C**), wound healing assay (**D**) and E-cadherin expression (**E**). E-cadherin localization was determined by immunofluorescence staining (green). Bar, 20 μm. Data in the graphs in (**B-D**) were derived from at least three independent experiments and are presented as means ± SEM [analysis of variance (ANOVA), Newman-Keuls multiple comparison test; $*P < 0.05$, $** P < 0.01$, $***P < 0.001$].

Figure S4

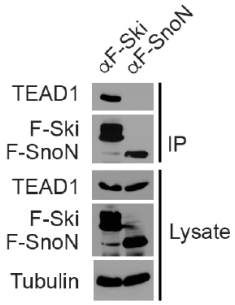

Figure S4, related to Figure 5. Ski, but not SnoN, interacts with endogenous TEAD1. F-SnoN or F-Ski was transfected into MCF10A cells, and endogenous TEAD1 associated with F-Ski or F-SnoN was isolated by immunoprecipitation with anti-Flag and detected by Western blotting with anti-TEAD1 antibodies (upper panels). The abundance of these proteins in the lysates was shown in the lower panels. Tubulin was used as a loading control.

Figure S5

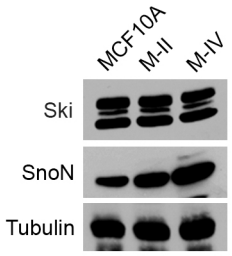

Figure S5, related for Figure 6. The levels of Ski do not change in MCF10A-derived breast cancer cell lines. Equal amounts of cell lysates were collected from MCF10A, M-II and M-IV cells and subjected to Western blotting to detect the expression levels of Ski and SnoN. Tubulin was used as a loading control.

Figure S6

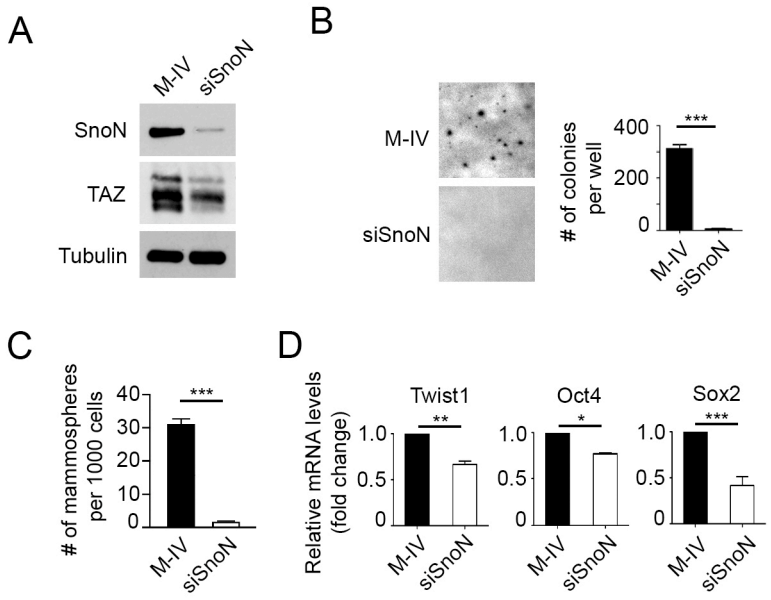

Figure S6, related for Figure 6. Reducing SnoN expression by siRNA impairs the oncogenic activities of M-IV cells. (**A**) The abundance of endogenous TAZ was reduced by siSnoN in M-IV cells. (**B**) Introduction of siSnoN impaired the anchorage-independent growth of M-IV cells. Soft agar colonies were stained and quantified in the graph (right). (**C**) Two-round mammosphere formation assay was carried out in M-IV cells expressing siSnoN. The numbers of mammospheres formed in the second round culture were counted, quantified and shown in the graph. (**D**) qRT-PCR analysis of breast cancer stem cell markers in M-IV cells expressing a scramble control or siSnoN. PCR values of Twist1, Oct4 and Sox2 were normalized to that of β-actin. Data in **B-D** were derived from at least three independent experiments and are shown as means ± SEM (two-tailed unpaired Student's t-tests, $*P < 0.05$, $** P < 0.01$, $***P < 0.001$).

Supplemental Experimental Procedures

Cell lines, antibodies and siRNAs

293T and HEK293 cells were cultured in Dulbecco's modified Eagle's medium (DMEM) supplemented with 10% fetal bovine serum and 100 U/ml penicillin/streptomycin (all from Invitrogen). The MCF10A and M-II mammary epithelial cells were cultured in DMEM/F12 1:1 medium supplemented with 5% horse serum, 20 ng/ml EGF, 10 μg/ml insulin, 0.5 μg/ml hydrocortisone and 100 ng/ml cholera toxin and penicillin/streptomycin. M-IV cells were cultured in DMEM/F12 1:1 medium plus 10% FBS.

Anti-SnoN (#4973) and anti-Mst2 were purchased from Cell Signaling. Anti-Lats2 was from Bethyl Laboratories. The antibodies against Sav, Mob, YAP, CTGF, Scribble and mouse SnoN (H317) was from Santa Cruz Biotechnology. Anti-E-cadherin and TEAD1 were from BD Transduction Laboratories and anti-TAZ and anti-GM130 (Golgi matrix marker) were from BD Pharmingen. Anti-Flag and anti-HA antibody were purchased from Sigma. The anti-Myc (9E10) was from Roche Diagnostics. The anti-Ski (G8) was from Cascade Bioscience. MAB 1378 (anti–α6-integrin) was purchased from Chemicon. Antibody against tubulin was from Calbiochem.

The following siRNAs were purchased from Dharmacom: human siWWTR1 (TAZ) SMARTpool, human siSKIL (SnoN) SMARTpool and scrambled non-Targeting siRNA Pool#2. siRNAs targeting Lats2 were purchased from Qiagen. siRNA targeting Scrib1 was purchased from Ambion.

Transfection, infection and immunoprecipitation

Stable MCF10A cells lines were generated by retroviral infection. Briefly, cDNAs or shRNAs in retroviral vectors were co-transfected with the packaging plasmids (pCMV-gag-pol and pBS-VSVG) into 293T cells using the Lipofectamine Plus transfection system (Invitrogen) to generated high-titer viral supernatant that was used subsequently to infect the MCF10A or M-IV cells. 48 h after infection, pools of infected cells were selected by growing in the presence of either 1.5 μg/ml puromycin or 0.2 mg/ml G418. siRNAs were transfected into cells using Lipofectamine RNAiMAX (Invitrogen) according to manufacturer's instructions.

For immunoprecipitation, briefly 6 μg of specific antibodies were pre-bound to 40 μl of protein A-Sepharose beads (Sigma-Aldrich) and incubated with 2-5 mg whole cell lysates in the lysis buffer (150 mM NaCl, 50 mM Hepes-KOH, pH 7.8, 5 mM EDTA, 0.1% NP-40, 3 mM dithiothreitol, and 0.5 mM PMSF) at 4 °C for at least 2 h. The isolated proteins were analyzed by Western blot with the indicated antibodies.

Immunofluorescence

Cells were fixed with 4% paraformaldehyde for 20 min, permeabilized with 0.1% Triton X-100 for 5 min and incubated with one of the following primary antibodies: anti-E-cadherin (1:300), anti-SnoN [rabbit polyclonal antibody against the peptide KELKLQILKSSKTAKE located at the C terminus of human SnoN, 1:2000; (Krakowski et al., 2005)], anti-TAZ (1:50), anti-YAP (1:200), anti-HA (1:2000), anti-Flag (1:5000), anti-Scrib (1:200) overnight at 4°C followed by staining with the appropriate Alexa fluorophore-conjugated secondary antibodies (Molecular Probes) for 1 h at room temperature. Cell nuclei were stained by DAPI staining.

Immunohistochemistry

Paraffin-embedded mouse mammary gland cross sections were deparaffinized in xylenes, rehydrated in a series of ethanol gradients, and permeabilized with 20 μg/ml proteinase K for 10 min at room temperature, according to a protocol that was described previously (Jahchan et al., 2010). Anti-TAZ staining was performed using the Tyramide Signal Amplification Biotin System kit (PerkinElmer) with anti-TAZ at 1:150. For visualization, DAB was used as the peroxidase substrate (SK-4105; Vector Laboratories). All images were visualized under a fluorescence microscope (AxioImager M2; Carl Zeiss).

Transwell migration assays

Cell migration was measured using the Transwell chambers (Corning). $1x10^5$ cells in medium with 1% FBS were seeded onto the collagen-coated membranes in the top chambers and allowed to migrate towards the bottom chambers filled with medium containing 10% FBS. Migrated cells were stained with 1% crystal violet in 20% methanol for 5 min and photographed. The number of migrated cells was scored

by counting the stained cells from multiple randomly selected visual fields under the microscope.

***In vitro* kinase Assay**

Flag-Lats2/Mst2 kinases were isolated by immunoprecipitation from transfected 293T cells with anti-Flag and subjected to an in vitro immune complex kinase assay using 4 μg GST-TAZ as an exogenous substrate in the presence of 5 μCi γ-P^{32}-ATP at 30°C for 30 min as described previously (Rashidian et al., 2015). The phosphorylated GST-TAZ was analyzed by SDS-polyacrylamide gene electrophoresis and visualized by autoradiography.

Quantitative RT-PCR (qRT-PCR)

Total RNA from MCF10A or M-IV cells was extracted using the RNeasy Mini kit (QIAGEN). Complementary DNA (cDNA) was produced by reverse transcription (SuperScript II; Invitrogen), using the gene-specific primers (see Supplemental experimental procedures, qRT-PCR primers) at a final concentration of 0.2 M. For semi-quantitative PCR, the following PCR program was performed: 95°C for 5 min (initial denaturation), 94°C for 30 sec, 55°C for 30 sec, and 72°C for 45 sec. Within the linear range of amplification, all PCR products were prepared under appropriate cycling conditions and separated on a 1% agarose gel. qRT-PCR was performed with the ABI 7300 (Applied Biosystem) per manufacturer's instruction. All PCR reactions were performed in duplicate in three independent experiments.

Statistical Analysis

All data were derived from at least three independent experiments and are presented as means ± SEM. Comparisons between two groups were performed by two-tailed unpaired Student's t-tests. Comparisons among three or more groups were performed by one-way ANOVA (Newman-Keuls multiple comparison test) with Prism 5 software. p values are shown when relevant ($*p < 0.05$; $**p < 0.01$, $***p < 0.001$).

qRT-PCR primers

Gene	Forward	Reverse
Mouse TAZ	CATGGCGGAAAAAGATCCTCC	GTCGGTCACGTCATAGGACTG
Mouse SnoN	CTTAGATGACTATGGAGATGCATC	GGTTCACATGAAGGTAACAGTGC
Mouse β-actin	CCAACCGTGAAAAGATGACC	CCATCACAATGCCTGTGGTA
TAZ	CCAGCCAAATCTCGTGATGAA	CGCATTGGGCATACTCATGA
GAPDH	CGTCTTCACCACCATGGAGA	CGGCCATCACGCCACAGTTT
Twist1	GAAAAGCGAGACAGGCCCGTG	GATTGGCACGACCTCTTGAG
Oct4	CGGAGGAGTCCCAGGACATCA	TGGTCGTTTGGCTGAATACCTT
Sox2	GCCGAGTGGAAACTTTTGTCG	GGCAGCGTGTACTTATCCTTCT
β-actin	GATCATTGCTCCTCCTGAGC	ACTCCTGCTTGCTGATCCAC

Supplemental References

KRAKOWSKI, A. R., LABOUREAU, J., MAUVIEL, A., BISSELL, M. J. & LUO, K. 2005. Cytoplasmic SnoN in normal tissues and nonmalignant cells antagonizes TGF-beta signaling by sequestration of the Smad proteins. *Proc Natl Acad Sci U S A,* 102**,** 12437-42.

RASHIDIAN, J., LE SCOLAN, E., JI, X., ZHU, Q., MULVIHILL, M. M., NOMURA, D. & LUO, K. 2015. Ski regulates Hippo and TAZ signaling to suppress breast cancer progression. *Sci Signal,* 8**,** ra14.